Journal of the European Ceramic Society **18** (1998) 237–240

PII: S0955-2219(97)00123-4
0955-2219/98/$19.00 + 0.00

Effect of Niobia on the Defect Structure of Yttria-stabilized Zirconia

Xin Guo* and Zhu Wang

State Key Laboratory for Synthesis and Processing of Advanced Materials, Wuhan University of Technology, Wuhan, Hubei Province 430070, People's Republic of China

(Received 17 March 1997; accepted 16 June 1997)

Abstract

Up to 1·0 mol% Nb_2O_5 was added to 9 mol% Y_2O_3-stabilized ZrO_2. The bulk resistivities were measured by the complex impedance approach, the additions of Nb_2O_5 were found to increase the resistivities. The defect structure change caused by the additions of Nb_2O_5 was studied by the positron annihilation technique (PAT), it was found that the additions of Nb_2O_5 can decrease the $V_{\ddot{O}}$ concentration and increase the $(Y'_{Zr}V_{\ddot{O}}Y'_{Zr})^x$ concentration, and possibly decrease the mobility of $V_{\ddot{O}}$, which explains the increasing bulk resistivities. The additions of Nb_2O_5 are expected to suppress the formation of defect associates, however, only adverse experimental results were found, suggesting that such kind of defect reactions are impossible in the low Nb_2O_5 concentration of the present work. © *1997 Elsevier Science Limited.*

1 Introduction

When a trivalent oxide, e.g. Y_2O_3, is added to ZrO_2 as stabilizer, certain amount of lattice defects, e.g. oxygen vacancies $V_{\ddot{O}}$ and negatively-charged solutes Y'_{Zr}, are produced in the ZrO_2 lattice. The conductivity of stabilized-ZrO_2 is determined by its defect structure, chiefly including $V_{\ddot{O}}$, Y'_{Zr} and the defect associates between them in the case of Y_2O_3-stabilized ZrO_2 (YSZ). Pentavalent oxides are positively charged, opposite to the stabilizers, when dissolved in the ZrO_2 lattice, the addition of pentavalent oxides in the stabilized-ZrO_2 will definitely affect the original defect structure, thus also the properties of the stabilized-ZrO_2. Ta_2O_5[1–3] has been found to affect the phase stability and the electrical properties of ZrO_2, and Nb_2O_5 has also been found to dramatically change the grain-boundary conductivity of ZrO_2.[4] Some attempts have been made to illustrate the defect structure changes involved in these phenomena,[4,5] however, a direct study of the defect structure change is still lack, thus this will be the subject of present work.

The positron annihilation technique (PAT) has been proved to be a useful tool for studying the defect structure in metals and ceramics.[6,7] Perhaps due to the complexity of ceramics, there are few positron annihilation studies until recently. The recent applications of PAT in La-doped $BaTiO_3$ [8] and other ceramics,[9,10] have shown that the positron annihilation is very sensitive to vacancy-type defects in ceramics, and PAT has been recently successfully used in the study of the defect structure change involved in the solid-state sintering of YSZ[11] by one of the authors. In the present work, the effect of Nb_2O_5 on the defect structure of YSZ will be studied via PAT. As the grain-boundary properties have been studied in Ref. 4, and the defect structure change usually produces the most immediate effect on bulk properties, the present work thus concerns only the bulk resistivities. The Kröger–Vink notation is used throughout this paper.

2 Experimental

The compositions of specimens are listed in Table 1. The starting materials are ZrO_2 with a purity of 99·5 wt%, Y_2O_3 with a purity of 99·99 wt% and Nb_2O_5 with a purity of 99·5 wt%. The specimens were prepared by the conventional ceramic processing method which involves mixing, ball-milling, pressing and sintering at 1500°C for 2 h. For electrical measurement, silver electrodes were applied by painting.

The resistances of the specimens were measured via the complex impedance approach in a

*To whom correspondence should be addressed.

Table 1. Compositions of specimens

Specimen	*Composition*
0NbYZ	ZrO_2–9 mol% Y_2O_3
0·5NbYZ	ZrO_2–9 mol% Y_2O_3–0·5 mol% Nb_2O_5
1·0NbYZ	ZrO_2–9 mol% Y_2O_3–1·0 mol% Nb_2O_5

Table 3. Positron lifetime parameters

Specimen	$\tau_1(ps)$	$I_1(\%)$	$\tau_2(ps)$	$I_2(\%)$	$\tau_a(ps)$
0NbYZ	181·3	94·5	407·3	5·5	193·8
0·5NbYZ	182·8	95·1	423·2	4·9	194·5
1·0NbYZ	183·6	95·3	420·8	4·7	194·7

frequency range of 20–1 MHz with a HP4285A precision LCR meter, and the bulk resistances were separated out by the analyses of the complex impedance plots according to the equivalent circuit initially proposed by Bauerle.[12]

The measurements of positron lifetime spectra were carried out at room temperature by a fast–fast coincidence lifetime spectrometer with a resolution (FWHM) of 262 ps. A 15 μCi ^{22}NaCl positron source was used in the measurements. A normal specimen–source–specimen sandwich arrangement was adopted, and a total of 10^6 counts in each spectrum was collected. After subtracting the source and background contribution, all lifetime spectra were analyzed with two components by the program POSITRONFIT EXTENDED.

3 Results

The bulk resistances of the specimens R_b measured at 450 and 500°C are given in Table 2. Every R_b value is the average one of three measurements. In order to eliminate the dimensional effect of the specimens, the corresponding bulk resistivities ρ_b are calculated from $\rho_b = R_b(s/l)$, where s/l is the cross-section/length ratio of the specimens. The ρ_b values are also given in Table 2, and ρ_b increases with increasing Nb_2O_5 content.

The positron lifetimes τ_1 and τ_2, and their relative intensities I_1 and I_2 are given in Table 3. The average lifetimes τ_a are calculated according to $\tau_a = \tau_1 I_1 + \tau_2 I_2$, they are also given in Table 3. The long life time component τ_2, whose intensity is very small, about 5·0%, most probably arises from the positron annihilation in the positron source and the pores in the specimens, so τ_2 can be neglected in the present work. τ_a reflects the comprehensive effect of every factors in the positron annihilation measurement. As shown in Table 3, the τ_1 and τ_a have the same changing tendency, though different values, τ_1 thus reflects the comprehensive effect of every factors in the specimens. τ_1 and I_1 increase slightly with increasing Nb_2O_5 content.

Table 2. Electrical data of the specimens

Specimen	*450°C*		*500°C*	
	$R_b(\Omega)$	$\rho_b(\Omega\,cm)$	$R_b(\Omega)$	$\rho_b(\Omega\,cm)$
0NbYZ	1050	4596	330	1444
0·5NbYZ	1140	5288	330	1526
1·0NbYZ	2500	7612	807	2456

4 Discussion

The lattice defect in YSZ are the grain boundaries and point defects. The major point defects in YSZ are Y'_{Zr} and $V_O^{\cdot\cdot}$. However, $V_O^{\cdot\cdot}$ will repulse positrons due to its positive charge. Because of coulombic interaction between the charged defects, some defect associates may be formed. It has been proved that $(Y'_{Zr}V_O^{\cdot\cdot})^{\cdot}$ is the dominant defect associate in dilute Y_2O_3 and ZrO_2 solution; in ZrO_2 with high Y_2O_3 concentration, the formation of $(Y'_{Zr}V_O^{\cdot\cdot}Y'_{Zr})^x$ is possible.[13–16] The formation of defect associates in CeO_2–Y_2O_3 solid solution has also been proposed.[17] The formation of defect associates binds some $V_O^{\cdot\cdot}$ to the Y'_{Zr} sites, making $V_O^{\cdot\cdot}$ unavailable for the conduction purpose. The positively charged defects will repulse positrons, so PAT is only sensitive to $(Y'_{Zr}V_O^{\cdot\cdot}Y'_{Zr})^x$ in YSZ. The above defect reactions can be summarized as follows

$$Y_2O_3 \rightarrow 2Y'_{Zr} + V_O^{\cdot\cdot} + 3O_o^x \qquad (1)$$

$$Y'_{Zr} + V_O^{\cdot\cdot} \rightarrow (Y'_{Zr}V_O^{\cdot\cdot})^{\cdot} \qquad (2)$$

$$(Y'_{Zr}V_O^{\cdot\cdot})^{\cdot} + Y'_{Zr} \rightarrow (Y'_{Zr}V_O^{\cdot\cdot}Y'_{Zr})^x \qquad (3)$$

In these defect reactions, the resulted defects of anterior reactions are the starting defects of posterior reactions.

The grain boundaries of an ionic crystal can be described as a double layer-like structure with an interface region and adjoined space-charge region. The interface region may carry an electric potential resulting from the presence of excess ions of one sign, and this potential is compensated by the space-charge region with opposite sign. The grain boundaries of YSZ have been studied by one of the authors,[4,18–21] the defect structure at the grain boundaries can be schematically presented as

Fig. 1. The space-charge potential in YSZ is proved to be negative, which corresponds to an Y'_{Zr} segregation and an $V_O^{\cdot\cdot}$ depletion in the space-charge region, whereas the potential of the interface region should be positive to compensate the negative space-charge potential. The addition of Nb_2O_5 does not dramatically change the grain–boundary defect structure of YSZ,[4] because the positively-charged grain–boundary interface prevents the segregation of niobium to the grain boundaries. The positively-charged grain–boundary interfaces will surely repulse positrons, and as the $V_O^{\cdot\cdot}$ concentration is very low in the space-charge region, the formation of $(Y'_{Zr}\ V_O^{\cdot\cdot}\ Y'_{Zr})^x$ is highly impossible, the space-charge region will thus also repulse positrons. As a result, the grain boundaries make no contribution to the PAT measurement results, i.e. τ_1 and I_1 reflect essentially the effect of the defect associates in the bulk. The slightly increasing τ_1 and I_1 shown in Table 3 means that the concentration of $(Y'_{Zr}\ V_O^{\cdot\cdot}\ Y'_{Zr})^x$ increases slightly with Nb_2O_5 content.

The same as Y_2O_3, Nb_2O_5 can only be substitutionally dissolved in ZrO_2, because it is obviously impossible to be interstitially dissolved when considering the relatively large radius of Nb^{5+} with respect to the interstices in the ZrO_2 lattice. According to a former work of one of the authors,[4] the most probable dissolving mechanism of Nb_2O_5 in ZrO_2 is

$$Nb_2O_5 \rightarrow 2Nb_{Zr}^{\cdot} + 2e + 4O_O^x + 1/2O_2 \qquad (4)$$

The addition of Nb_2O_5 does not introduce new positron-sensitive defect into YSZ, but introduces 2 mol% free electrons for every molar fraction of Nb_2O_5. The free electrons thus produced may annihilate $V_O^{\cdot\cdot}$ by the following defect reactions

$$2e + V_O^{\cdot\cdot} \rightarrow (2eV_O^{\cdot\cdot})^x \qquad (5a)$$

or

$$2e + V_O^{\cdot\cdot} \rightarrow \text{null} \qquad (5b)$$

so the $V_O^{\cdot\cdot}$ concentration in the specimens with Nb_2O_5 additions is reduced. If the annihilation of $V_O^{\cdot\cdot}$ is accomplished by the formation of color centers $(2e\ V_O^{\cdot\cdot})^x$, which will induce the color of brown or gray in the specimens,[22,23] then the color of the specimens with Nb_2O_5 additions should not be white. However, this is not the case. Therefore, the annihilation of $V_O^{\cdot\cdot}$ should be accomplished according to eqn (5b). The annihilation of $V_O^{\cdot\cdot}$ can also be explained by the compensation effect between the acceptor (Y_2O_3) and the donor (Nb_2O_5).[5,24] According to eqn (2), the concentration of $(Y'_{Zr}\ V_O^{\cdot\cdot})^{\cdot}$ is also reduced due to the reduced $V_O^{\cdot\cdot}$ concentration. The total concentration of Y'_{Zr}, according to eqn (1), should be 18 mol% in the 9 mol% Y_2O_3-stabilized ZrO_2, thus the Y'_{Zr} concentration after the reaction (2) should be $[Y'_{Zr}] = 18 - [(Y'_{Zr}\ V_O^{\cdot\cdot}]$, the square brackets indicating concentration. The reduced $[(Y'_{Zr}\ V_O^{\cdot\cdot})^{\cdot}]$ increases the $[Y'_{Zr}]$ in the reaction (3), this may increase the concentration of $(Y'_{Zr}\ V_O^{\cdot\cdot}\ Y'_{Zr})^x$, according to eqn (3). The slightly increasing τ_1 and I_1 show that this is just the case.

The addition of Ta_2O_5 or Nb_2O_5 to YSZ does not change the conduction mechanism.[34] The bulk conductivity $\sigma_b = 2e\mu[V_O^{\cdot\cdot}]$, μ is the mobility of $V_O^{\cdot\cdot}$, the reduced $[V_O^{\cdot\cdot}]$ surely increases the bulk resistivity. Nb^{5+} ion on the Zr^{4+} site implies a net effective charge of $+1$, which repels $V_O^{\cdot\cdot}$. This increases the difficulty of the $V_O^{\cdot\cdot}$ movement in the YSZ lattice, so the mobility decreases, which also increases the bulk resistivity. These two factors explain the increasing bulk resistivities shown in Table 2.

In addition, there may be another possible defect reaction involved in the Nb_2O_5 additions. Because of the expected repulsive force between $Nb_{Zr}^{\cdot}$ and $V_O^{\cdot\cdot}$, the introduction of $Nb_{Zr}^{\cdot}$ into YSZ may suppress the formation of the defect associates, even split the already formed defect associates, i.e. two defect reactions defined as follows may occur

$$(Y'_{Zr}\ V_O^{\cdot\cdot}\ Y'_{Zr})^x \xrightarrow{Nb_{Zr}^{\cdot}} (Y'_{Zr}\ V_O^{\cdot\cdot})^{\cdot} + Y'_{Zr} \qquad (6)$$

$$(Y'_{Zr}\ V_O^{\cdot\cdot})^{\cdot} \xrightarrow{Nb_{Zr}^{\cdot}} Y'_{Zr} + V_O^{\cdot\cdot} \qquad (7)$$

which will increase the concentration of mobile $V_O^{\cdot\cdot}$. This surely decreases the concentration of the only

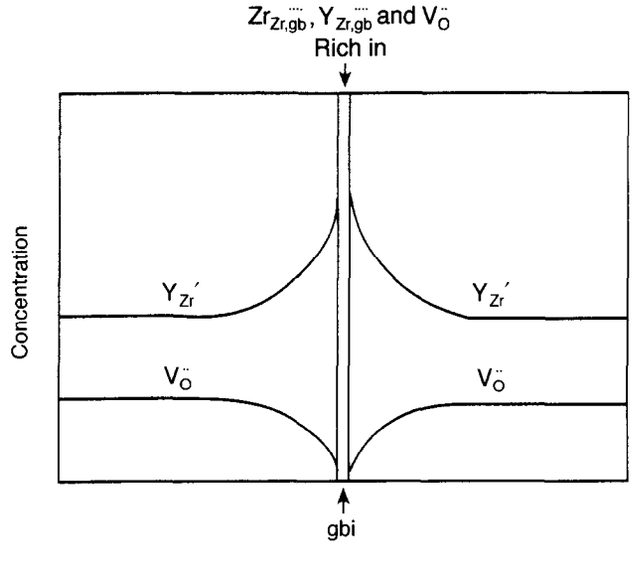

Fig. 1. Defect distribution in the grain–boundary interface (gbi) and the space-charge region of the YSZ specimen.[19]

positron-sensitive defect associate in YSZ: $(Y'_{Zr}\ V_O^{\cdot\cdot}\ Y'_{Zr})^x$. However, this certainly will also decrease τ_1 and I_1 and the bulk resistivities. From the experimental results, we can unequivocally see that such defect reactions are highly impossible, at least at the low Nb_2O_5 concentrations of the present work. This result is in accordance with the work of Choudhary and Subbarao.[3]

5 Conclusion

The additions of Nb_2O_5 to YSZ decrease the concentration and mobility of $V_O^{\cdot\cdot}$, as a result, the bulk resistivity increases. And the additions of Nb_2O_5 to YSZ also increase the formation probability of the defect associate $(Y'_{Zr}\ V_O^{\cdot\cdot}\ Y'_{Zr})^x$. Besides, the introduction of Nb_2O_5 into YSZ is expected to suppress the formation of the defect associates, however, the present work does not support such a postulation.

Acknowledgements

Project supported by the Natural Science Foundation of China and the Natural Science Foundation of Hubei Province.

References

1. Kim, D. J., Effect of Ta_2O_5, Nb_2O_5, and HfO_2 alloying on the transformability of Y_2O_3-stabilized tetragonal ZrO_2. *J. Am. Ceram. Soc.*, 1990, **73**, 115–120.
2. Kim, D. J. and Tien, T. Y., Phase stability and physical properties of cubic and tetragonal ZrO_2 in the system ZrO_2–Y_2O_3–Ta_2O_5. *J. Am. Ceram. Soc.*, 1991, **74**, 3061–3065.
3. Choudhary, C. B. and Subbarao, E. C., Electrical conduction in the cubic fluorite phase in the system ZrO_2–$YO_{1.5}$–$TaO_{2.5}$. In *Fast Ion Transport in Solids*, ed. P. Vashishta, J. N. Mundy and G. Shenoy. Elsevier North-Holland, New York, 1979, pp. 665–668.
4. Guo, X., Effect of Nb_2O_5 on the space-charge conduction of Y_2O_3-stabilized ZrO_2. *Solid State Ionics*, to be published.
5. Kountouros, P. and Petzow, G., Defect chemistry, phase stability and properties of zirconia polycrystals. In *Science and Technology of Zirconia V*, ed. S. P. S. Badwal, M. J. Bannister and R. H. J. Hannink. Technomic, Lancaster, Basel, 1993, pp. 30–48.
6. Brandt, W. and Dupasquier, A., *Positron Solid State Physics*. North-Holland, Amsterdam, 1983.
7. Brandt, W., Positron dynamics in solids. *Appl. Phys.*, 1974, **5**, 1–23.
8. Tang, C. Q., Nonmonotonic dependence of the positron lifetimes on the dopant content in La-doped $BaTiO_3$. *Phys. Rev. B*, 1994, **50**, 9774–9777.
9. Sanyal, D., Banerjee, D., Bhattacharya, R., Patra, S. K., Chaudhuri, S. P., Ganguly, B. N. and De, U., Study of transition metal ion doped mullite by positron annihilation techniques. *J. Mater. Sci.*, 1996, **31**, 3447–3451.
10. Dannefaer, S. and Kerr, D., Defects in CZ-silicon investigated by the positron annihilation techniques. In *Microscopic Identification of Electronic Defects in Semiconductors*, ed. N. M. Johnson, S. G. Bishop and G. D. Watkins. Materials Research Society, Pittsburgh, 1985, pp. 477–480.
11. Guo, X., Plausible role of point defects in the solid-state sintering of yttria-stabilized zirconia: a positron annihilation study. *J. Mater. Sci. Lett.*, 1996, **15**, 2017–2019.
12. Bauerle, J. E., Study of solid electrolyte polarization by a complex admittance method. *J. Phys. Chem. Solids*, 1969, **30**, 2657–2670.
13. Subbarao, E. C. and Maiti, H. S., Solid electrolytes with oxygen ion conduction. *Solid State Ionics*, 1984, **11**, 317–338.
14. Butler, V., Catlow, C. R. A. and Fender, B. E. F., The defect structure of anion deficient ZrO_2. *Solid State Ionics*, 1981, **5**, 539–542.
15. Mackrodt, W. C. and Woodrow, P. M., Theoretical estimates of point defect energies in cubic zirconia. *J. Am. Ceram. Soc.*, 1986, **69**, 277–280.
16. Yashima, M., Ishizawa, N. and Yoshimura, M., Application of an ion-packing model based on defect clusters to zirconia solid solutions: I, modeling and local structure of solid solutions. *J. Am. Ceram. Soc.*, 1992, **75**, 1541–1549.
17. Wang, D. Y. and Nowick, A. S., Dielectric relaxation from a network of charge defects in dilute CeO_2: Y_2O_3 solid solutions. *Solid State Ionics*, 1981, **5**, 551–554.
18. Guo, X., Solute segregations at the space-charge layers of stabilized zirconia: an opportunity for ameliorating conductivity. *Journal of the European Ceramic Society*, 1996, **16**, 575–578.
19. Guo, X., Physical origin of the intrinsic grain-boundary resistivity of stabilized-zirconia: role of the space-charge layers. *Solid State Ionics*, 1995, **81**, 235–242.
20. Guo, X. and Yuan, R. Z., On the grain boundaries of ZrO_2-based solid electrolyte. *Solid State Ionics*, 1995, **80**, 159–166.
21. Guo, X., Space-charge conduction in yttria and alumina codoped-zirconia. *Solid State Ionics*, 1997, **96**, 247–254.
22. Guo, X., Sun, Y. Q. and Cui, K., Darkening of zirconia: a problem arising from oxygen sensors in practice. *Sensors and Actuators*, 1996, **B31**, 139–145.
23. Guo, X., Effect of DC voltage on the microstructure and electrical properties of stabilized-zirconia. *Solid State Ionics*, 1997, **99**, 143–151.
24. Lu, H. Y. and Chen, S. Y., Sintering and compensation effect of donor- and acceptor-codoped 3 mol% Y_2O_3–ZrO_2. *J. Mater. Sci.*, 1992, **27**, 4791–4796.